Optical MEMS pressure sensor using ring resonator on a circular diaphragm

Prasant Kumar Pattnaik, Bh. Vijayaaditya, T. Srinivas and A. Selvarajan
Department of Electrical Communication Engineering
Indian Institute of Science, Bangalore 560012, India
Email: pattu@ece.iisc.ernet.in

Abstract

In this paper we propose and analyse an optical MEMS pressure sensor consisting of a ring resonator located over the edge of a circular silicon diaphragm. As the diaphragm deflects due to the applied pressure, stress induced refractive index change in the waveguide leads to change in phase of the light propagating through resonator. Shift in the resonance frequency due to this phase change gives the measure of the applied pressure. The phase response of the sensor is found to be about $19\mu rad/Pa$ for 1mm radius $65\mu m$ thick circular diaphragm. The wavelength shift of $0.78pm/kPa$ is obtained for this sensor and can be used upto a range of $300kPa$. Since the wavelength of operation is around $1.55\mu m$, hybrid integration of source and detector is possible on the same substrate. This type of sensor can be used for blood pressure monitoring, precession instrumentation, aerospace propulsion application and other harsh enviroments with suitable design.

1 Introduction

Micro-opto-electro-mechanical (MOEM) devices and systems, based on the principles of integrated optics and micromachining technology on silicon have immense potential for sensor applications [1]. Optical MEMS sensors have the advantages of immune to EMI, larger bandwidth and higher sensitivity compared to electronic counter parts. Many types of optical MEMS pressure sensors using Mach-Zehnder interferometer(MZI) [2, 3], Fabry-Perot interferometer [4] have been reported. Phase change in the sensing arm of MZI due to applied pressure is read out as intensity change in case of MZI baed sensor. In Fabry-Perot interferometer based pressure sensor, the variation of cavity length because of displacement of the diaphragm due to applied pressure is readout as intensity changes. Brabander et.al [5] have considered ring resonator based pressure sensor whose straight arms are over the long edge of a micromachined rectangular diaphragm. But here we consider a circular sil-

icon diaphragm and consider the resonant wavelength shift of the ring resonator as a measure of applied pressure.

2 Sensor Configuration

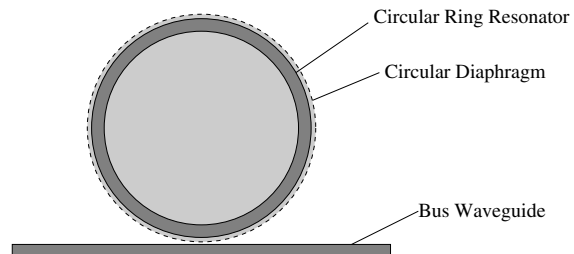Figure 1 shows the schematic of the sensor. When pres-

Figure 1. Schematic of the proposed Optical MEMS Pressure Sensor

sure is applied on the diaphragm, due to the stress in the waveguide located over the diaphram, the refractive index changes (due to elasto-optic effect) and hence the phase of the light propagating through it. This phase change is read out as resonant wavelength shift of the ring resonator located over the diaphragm. Since the waveguide is along the edge of the diaphragm where maximum stress occurs, phase change in the waveguide due to cumulative photoelsatic effect is more.

3 Ring Resonator

The ring resonator is located over the edge of the diaphragm as shown in figure 1. Light is coupled into and out of the ring from the straight waveguide placed adjcent to it over the substrate [6]. The ring is made up of oxinitride($SiO_2/SiON/SiO_2$) waveguide single moded at $1.55\mu m$. The ratio of the output and input field (I_t) is given

by

$$I_t = \left[\frac{(1-k^2)^{\frac{1}{2}} - exp\{-(\alpha_T + i\phi)\}}{1 - (1-k^2)^{\frac{1}{2}} exp\{-(\alpha_T + i\phi)\}} \right]^2 \quad (1)$$

where, k is the coupling coefficient, $\alpha_T = \alpha L$ is the total propagation loss in the ring, $\phi = \frac{2\pi}{\lambda} n_{eff} L$ and $L = 2\pi r$, where r is the radius of the ring. Figure 3 shows the in-
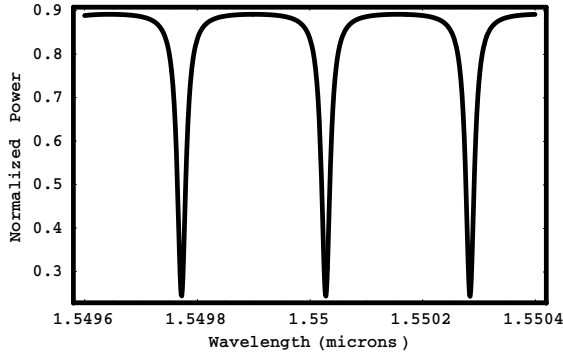

Figure 2. Output Charecteristics of the Ring Resonator

tensity variations at the output with the variation in the input wavelength with periodic dips at resonant wavelengths. Here r=1mm and $n_{eff} = 1.48789$ at 1550nm is taken for the desired waveguide structure with k=0.1% and very low loss ($\alpha \simeq 0$). As seen from the graph, the free spectral range (FSR) is about $257pm$.

4 Mechanical Design and Optomechanical Coupling

The deflection w of a circular diaphragm of radius 'a' and thickness h due to pressure P is given by

$$D\nabla^4 w(r) = P \quad (2)$$

where $D = \frac{Eh^3}{12(1-\nu^2)}$ is the flexural rigidity and E is the Youngs modulus and ν is the Poisson's ratio along with the boundary conditions

$$w(a) = 0 \quad w'(a) = 0 \quad w'(0) = 0 \quad (3)$$

The radial and transverse stress along the thickness of the diaphragm are given by

$$\sigma_r = \frac{Ez}{1-\nu^2} \left(\frac{\partial^2 w}{\partial r^2} + \nu \frac{\partial^2 w}{\partial t^2} \right)$$
$$\sigma_t = \frac{Ez}{1-\nu^2} \left(\frac{\partial^2 w}{\partial t^2} + \nu \frac{\partial^2 w}{\partial r^2} \right) \quad (4)$$

where r and t indicate radial and transverse direction. Hence the radial and tangential stresses at the surface of the circular diphragm ($z = \frac{h}{2}$) are given by

$$\sigma_r = \frac{3a^2}{8h^2} P \left[(3+\nu)\frac{r^2}{a^2} - (1+\nu) \right]$$
$$\sigma_t = \frac{3a^2}{8h^2} P \left[(1+3\nu)\frac{r^2}{a^2} - (1+\nu) \right] \quad (5)$$

Figure 3 shows the normalised stress($\frac{Pa^2}{h^2}$) variation along the diagonal of the diaphragm. The maximum radial stress
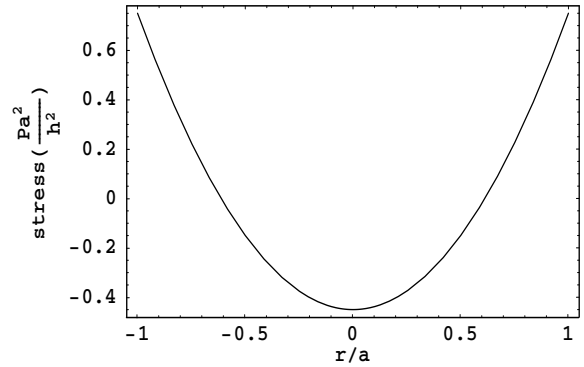

Figure 3. Normalised stress ($\frac{Pa^2}{h^2}$) along the diagonal of the diaphragm

occurs at the edge of the circular diaphragm and is $\frac{3a^2}{4h^2}P$. Hence the waveguide is placed at the edge to get the maximum refractive index change due to photoelastic effect. Larger radius and thinner diaphragm will have more stress for a given applied pressure. The radius of the diaphragm is chosen considering the ring radius which dictates the resonant wavelengths.

Due to the stress, the refractive index of the waveguide changes. Refractive index change is related to the stress through a fourth rank tensor called photoelastic tensor. There are only two nonzero coefficients C_1 and C_2 for the oxynitride core waveguide. The refractive index change is more for TM modes since the radial stress is more and is given by

$$\Delta n_{TM} = C_2 \sigma_r \quad (6)$$

where $C_2 = 4.22 \times 10^{-12}/Pa$ is the photoelastic coefficient of the core silicon oxynitride. Figure 4 shows the index change along the diameter for TM modes.
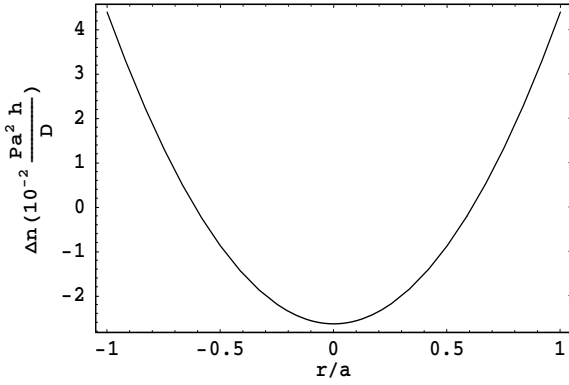
Figure 4. Normalised refractive index change ($\frac{Pa^2h}{D}$) along the diagonal of the diaphragm

5 Results

The cumulative phase change along the edge of the diaphragm is given by

$$\Delta\phi = \frac{2\pi}{\lambda}\frac{n}{n_{eff}}\Delta n\,(2\pi a) \tag{7}$$

Substituting for Δn, we get

$$\Delta\phi = \frac{2\pi}{\lambda}\left(\frac{n}{n_{eff}}\right)C_2\left(\frac{3a^2}{4h^2}\right)(2\pi a)P \tag{8}$$

Figure 5 shows the cumulative phase change for $1mm$ radius ring for various applied pressure. The phase sensitivity
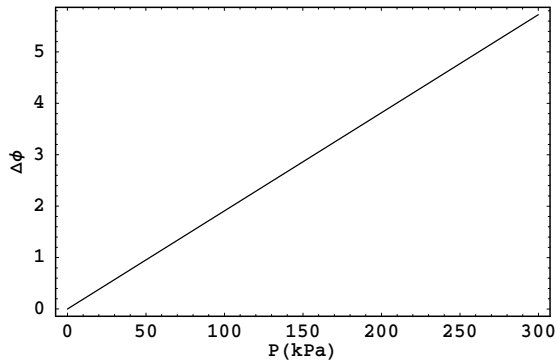

Figure 5. Phase change in the resonator due to applied pressure

here is about $19\mu rad/Pa$ for diaphagm thickness of $65\mu m$.

Since maximum allowable phase change can be 2π, about $300kPa$ can be detected. The free spectral range (FSR) in terms of wavelength is

$$\Delta\lambda_{FSR} = \frac{\lambda^2}{2\pi n_{eff}a} \tag{9}$$

Hence the wavelength shift due to applied pressure can be written as

$$\Delta\lambda_{Shift} = \Delta\lambda_{FSR}\frac{\Delta\phi(P)}{2\pi} \tag{10}$$

Figure 6 shows the variation of the intensity versus input wavelength for an applied pressure of $100kPa$. The dotted curve shows the variations without any applied pressure. It is obseerved from the graph that there is a resonant wavelength shift of $78pm$ for $100kPa$. Figure 7 shows the plot
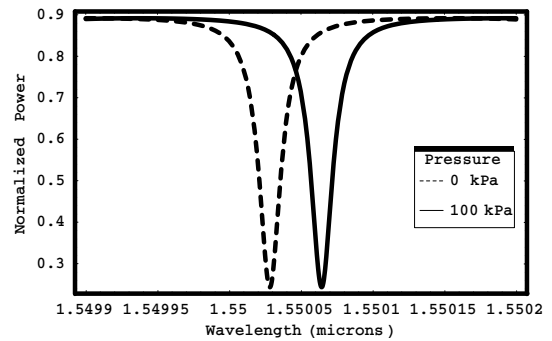

Figure 6. Intensity vs Wavelength for 0 and $100kPa$

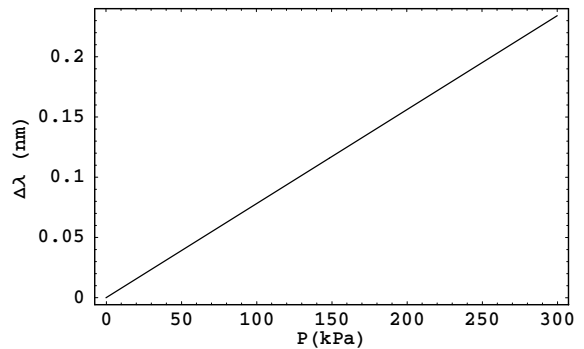of wavelength shift with pressure upto $300kPa$ which is the maximum detectable range for the proposed design. The

Figure 7. Resonant wavelength Shift vs Pressure

IEEE
COMPUTER
SOCIETY

plot shows linear varition in the shift with pressure which is desirable for sensor applications. In the present design, the diaphragm thickness is taken to be $65\mu m$. However by reducing the thickness (e.g $10\mu m$), one can achieve better sensitivity ($32pm/kPa$), for low pressure ($7.5kPa$) sensing applications.

6 Conclusion

We have proposed and analysed a novel optical MEMS pressure sensor using integrated optical ring resonator over a micromachined silicon circular diaphragm. Because the frequency of operation is around $1.55\mu m$, hybrid integration of source and detector is possible on the same substrate. Since the detection of pressure is in frequency domain, it is less amenable to noise. We have designed the sensor for $300kPa$ range. But with suitable modification in the design parameters, this sensor can be used for blood pressure monitoring, precession instrumentation, aerospace propulsion application and other harsh enviroments.

Acknowledgments

References

[1] M.Tabib Azar and G.Behelm , Modern trends in microstructures and integrated optics for communication, sensing and signal processing, *Opt. Engg.*, 36(5):1307-1318 ,May 1997.

[2] M.Ohkawa, M.Izustu and T.Sueta, Integrated Optic Pressure Sensor on silicon substrate, *Appl. Opt.* ,28(23):5153-5157, December 1989.

[3] Prasant Kumar Pattnaik, A. Selvarajan and T.Srinivas, Guided wave optical MEMS pressure sensor, *Proc. of ISA/IEEE Conference on Sensors for Industry SIcon/05*, pp.122-125, February 8-10, 2005, Houston, Texas, USA.

[4] Y. Kim and D.P.Neikrik, Micromachinded fabry-perot cavity pressure sensor, *Photon. Technol. Lett.*, 7(12):1471-1473, December 1995.

[5] G.N.De Brabender, J.T.Boyd and G.Beheim, Integrated Optical Ring Resonator With Micromechanical Diaphragm for Pressure Sensing, *Photon. Technol. Lett.*,6(5):671-673, May 1994.

[6] B.E.Little, S.T.Chu,H.Aa.Haus,J.Foresi and J.P.Laine, Microring resonator channel droping filters, *Jl. of Lightwave Technol.*,15(6):998-1005, June 1997.